

*promoting access to White Rose research papers*



**Universities of Leeds, Sheffield and York**  
**<http://eprints.whiterose.ac.uk/>**

---

This is the author's post-print version of an article published in **Journal of Materials Processing Technology**

White Rose Research Online URL for this paper:

<http://eprints.whiterose.ac.uk/id/eprint/78688>

---

**Published article:**

Mullis, AM, McCarthy, IN and Cochrane, RF (2011) *High speed imaging of the flow during close-coupled gas atomisation: Effect of melt delivery nozzle geometry*. Journal of Materials Processing Technology, 211 (9). 1471 - 1477. ISSN 0924-0136

<http://dx.doi.org/10.1016/j.jmatprotec.2011.03.020>

---

# High Speed Imaging of the Flow During Close-Coupled Gas Atomisation: Effect of Melt Delivery Nozzle Geometry

A.M. Mullis<sup>†</sup>, I.N. McCarthy & R.F. Cochrane  
Institute for Materials Research, University of Leeds, Leeds LS2-9JT, UK

## Abstract

We describe the application of a high-speed still imaging technique to the study of close-coupled gas atomisation. A pulsed Nd:YAG laser is used to obtain pairs of still images with an effective 6 ns exposure time, from which velocity maps of the flow of the atomised fluid can be reconstructed. We demonstrate directly that the melt spray cone consists of a jet precessing around the surface of a cone. Further, we demonstrate that the width of this jet is directly related to the geometry of the melt nozzle. By applying Particle Image Velocimetry techniques we are also able to map the flow field in both the primary and secondary atomisation zones, demonstrating an asymmetric recirculation eddy exists at the circumferential edge of the gas-melt interface in the primary atomisation zone.

**Keywords:** Gas atomisation; Discrete Fourier transform; Particle Image Velocimetry

## Introduction

Close-coupled gas atomisation (CCGA) is an important production technique for fine, spherical metal powders. Such powders have a variety of uses, such as for pigments, catalysts, metal injection moulding (MIM) feedstock, solder pastes for 'flip-chip' type circuit board fabrication and solid rocket propellant. In principle, CCGA is straightforward: high pressure gas jets impinging upon a molten metal stream are used to disrupt the stream, breaking it up into a series of fine droplets. However, in practice the complex interaction between the high velocity gas jets and the metal results in a turbulent, and often chaotic, flow with the result that the details of the process are far from well understood. Consequently, early work into gas atomisation, such as that by Klov and Schfer (1972) or Bradley (1973), focused on empirical correlations between median particle size and process parameters such as gas pressure, gas flow rate and melt flow rate. The most widely quoted of these empirical relationships is that due Lubanska (1970), which correlates particle size with  $(1+G)^{1/2}$ , where  $G$  is the mass ratio of metal flow to gas flow.

Many notable advances in atomiser design have been brought about in recent years through the careful, scientific study of the atomisation process. These have allowed significant progress to be made towards understanding a number of factors that may influence both median particle size and standard deviation. Despite this, a significant problem with CCGA remains the wide distribution of particle sizes produced. This contrasts with many end-users specification for a tightly constrained distribution, which necessitates significant sieving and classification to obtain the in-specification product, so reducing the yield of the process. As pointed out by Nasr et al. (2002), remelting of the remaining product can add substantially to the cost and energy usage of the overall process.

Recently Mates and Settles (1996) have demonstrated that high speed imaging, either of just the gas flow-field using techniques such as Schlieren imaging, or direct imaging of the melt plume, can allow significant progress to be made towards understanding a number of factors that may influence the particle size distribution. A number of advances in atomiser design have followed from such studies, including modifications to the internal geometry of the melt delivery nozzle, increased interest in discrete jet, as opposed to annular slit, designs for the gas delivery die (Unal, 2007) which significantly reduce gas consumption at elevated pressure and convergent-divergent (de Laval) geometry gas jets (Unal, 1989). As demonstrated by Anderson et al. (2002), this latter modification permits the gas to expand to

---

<sup>†</sup> Corresponding author: e-mail [a.m.mullis@leeds.ac.uk](mailto:a.m.mullis@leeds.ac.uk), tel +44-113-343-2568, fax +44-113-343-2384.

ambient pressure in a shock free manner thus allowing flow at high Mach number and reducing energy loss from the gas. With regard to the melt delivery nozzle, Anderson et al. (2004) have shown the internal profiling of the nozzle can be the determining factor in how well the melt is disrupted in the primary atomisation zone. Common designs include a simple flat tip, some degree of internal tapering, and concave designs (Miller, 1986), which may be used to deflect the recirculating gas, which has been claimed to increase the coupling between the gas and the melt (Miller; 1986). More complex designs such as the Bessel horn have also been used (Anderson et al., 2004), again on the principle of improving the gas-melt coupling.

The analysis of high speed imaging has proved to be particularly fruitful when combined with Fourier analysis of the resulting images. Ting et al. (2005) noted that during CCGA the atomiser plume oscillated in two characteristic frequency ranges, a low frequency range (dominant around 10 Hz) and a high frequency range (dominant around 1200 Hz). The low frequency oscillation appeared to be related to pulsation in the quantity of material discharged at the tip of the melt delivery nozzle. This effect, which it is thought arises as the gas flow alternates between open- and closed-wake conditions, will result in fluctuations in  $G$  on short time-scales. This will in turn lead to a widening of the particle size distribution. The mechanism behind the second, higher frequency oscillation was more elusive, although it was postulated that this might be related to the melt disintegration process.

In two recent papers (Mullis et al., 2008; McCarthy et al., 2009) we have reported the results of a series of experiments in which high-speed (18,000 fps) video imaging was used to study both a research scale metal atomiser and an analogue (water) atomiser. In the case of the metal atomiser the material being atomised was a Ni-Al alloy with an initial melt temperature of  $\sim 1800$  K, wherein the melt plume had sufficient luminosity to be imaged without additional light sources being employed. For the water atomiser, the plume was imaged in reflected light provided by two high power halogen lamps. The resulting images were quantitatively analysed by considering the volume of material in the plume and the position of the plume centre as the material passed through a narrow window, 2 nozzle diameters below the atomisation tip. For each film sequence two time-series were thus produced, detailing the variation with time of the volume of material being atomised and the centre position of the plume. A Discrete Fourier Transform (DFT) was subsequently applied to each time-series to determine any dominant frequencies present (see Mullis et al., 2008; McCarthy 2010 for a full description of the analysis methodology).

Like Ting et al. (2005) dominant modes of oscillation were observed at both low and high frequencies. The low frequency oscillation, which appeared only in the intensity and not in the position spectra, could clearly be associated with pulsing in the volume of material at the atomisation tip, which can be accounted for by the open- to closed-wake model proposed by Ting et al. (2005). In contrast, the high frequency oscillation appeared in both spectra with exactly the same frequency and was therefore indicative of a displacement of the plume, as well as a variation in the apparent brightness of the material in the plume. In fact, careful analysis of the raw time-series data revealed that the maxima (minima) in the intensity time-series were exactly  $90^\circ$  out of phase with the maxima (minima) in the position time-series. This was inferred to be due to the melt plume consisting of a thin jet that was precessing around the surface of a cone, with the maxima and minima in the intensity corresponding to the jet being aligned with the line-of-sight to the camera. Figure 1 shows a schematic diagram illustrating this motion. Anderson et al. (2006) has also previously observed partial wetting of the melt delivery nozzle, although they comment on the wetting pattern being irregular, whereas Mullis et al., (2008) observed a highly regular rotation.

Moreover, Mullis et al., (2008), noted significant variations in the nature of the high frequency component of the DFT spectra as a function of nozzle geometry. In particular, nozzles with a broad, flat tip (see Fig. 2 below) gave a wide, rather diffuse spectra containing many frequencies, while nozzles with some level of internal tapering gave spectra which were

much more sharply peaked around the precession frequency. Mullis et al. conjectured that such a sharply defined peak implied a more regular precessional motion, although a precise interpretation of this data is difficult without more detailed knowledge of the melt filament geometry as a function of nozzle type. Indeed, even the conclusion regarding precession of the melt from these experiments remains an inference, rather than a direct observation.

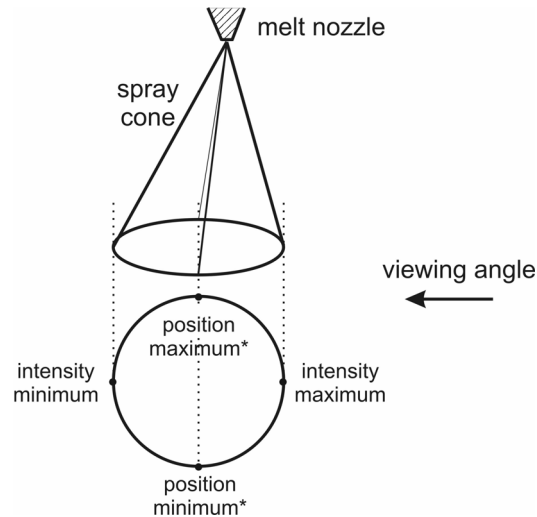


**Figure 1.** Schematic model showing how precession of a melt filament around the surface of a cone could give rise to variation in the intensity and position of the apparent melt plume that are exactly  $90^\circ$  out of phase. \*Note that the position maxima and minima may be interchanged depending upon the pixel number scheme [after Mullis et al.,2008].

The purpose of this paper is to describe a set of experiments with an alternative imaging system that allows direct observation of precession within the melt plume. Such direct observation offers the prospect of being able to significantly improve the extent to which it is possible to interpret the DFT spectra from the results presented by Mullis et al., thus aiding our understanding of how different internally profiled melt nozzles affect the interaction between the gas and melt during close-coupled atomisation.

### Experimental Technique

Imaging experiments were conducted on an analogue atomiser which utilises a simple die of the discrete jet type with 18 cylindrical jets arranged around a tapered melt delivery nozzle at an apex angle of  $45^\circ$ . The design, which is shown schematically in Fig. 2a, is similar to the USAG (Anand et al., 1978) and Ames HPGA-I (Anderson et al., 1991) designs. Although these designs are known to be sub-optimal in their atomisation performance, the cylindrical jets giving rise to choked flow which limits the outlet gas velocity to Mach 1, we have used this geometry as it has been discussed extensively in the literature. Four different melt delivery nozzles were used in this study and they are shown schematically in Fig. 2b, these may be described as; flat tipped, flared with lip, flared without lip and hemispherical respectively. The atomiser was used at an inlet gas pressure of 2 MPa, although it has been shown elsewhere that the frequency of precession of the melt is essentially independent of the gas inlet pressure (measured in the range 1-6.5 MPa).

Prior to imaging experiments being conducted the aspiration characteristics of the analogue atomiser have been established as a function of both inlet gas pressure (in the range 0.5-5 MPa) and nozzle geometry. This was measured in gas only flow by inserting a fine capillary down the melt delivery tube. The capillary was located 3 mm above the end of the melt delivery nozzle so that it did not protrude into the tapered region of the nozzle for any of the geometries used, thus not interfering with the gas flow patterns. The end of the capillary was connected to a manometer giving the differential pressure between the melt delivery

tube and the ambient pressure in the enclosure. The pressure difference was recorded with a time resolution of 0.1 s but here the time averaged pressure is reported, with averaging occurring over a period of 10 s, this timeframe being much longer than the characteristic timescales on which atomiser behaviour fluctuates and which is therefore sufficient to smooth such fluctuations.

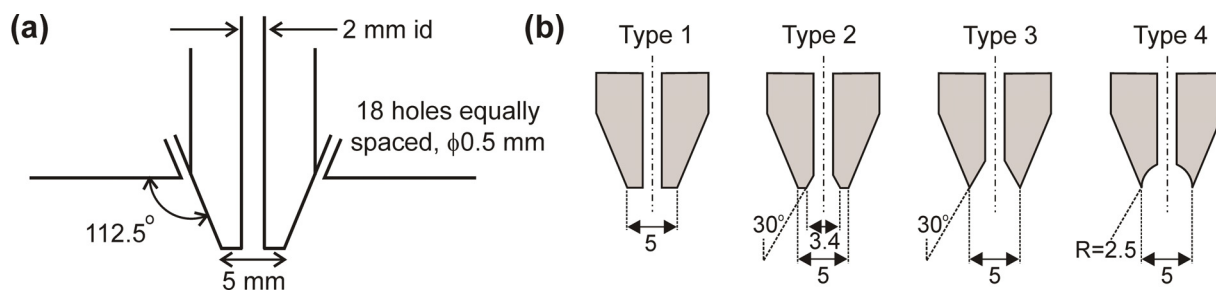


**Figure 2.** Schematic geometry of the gas delivery jets and melt delivery nozzles used in this study.

In most cases imaging experiments have been performed using deionised water. However, in order to investigate the effect of surface tension on the resulting spray, one set of experiments has been conducted with the addition of the surfactant sodium dodecyl sulphate (SDS), also widely referred to as sodium lauryl sulphate, a commercial surfactant widely used in cleaning and hygiene products. Use of SDS gives access to values of the surface tension,  $\sigma$ , in water between  $72 \text{ mN m}^{-1}$  at zero concentration to  $\sim 30 \text{ mN m}^{-1}$  in the fully saturated solution. Analogue atomisation experiments have been conducted at SDS concentrations corresponding to values for the surface tension of  $72 \text{ mN m}^{-1}$ ,  $67 \text{ mN m}^{-1}$ ,  $50 \text{ mN m}^{-1}$ ,  $43 \text{ mN m}^{-1}$  and  $36 \text{ mN m}^{-1}$ . The dependence of  $\sigma$  upon concentration of SDS is given by a number of sources [see e.g. Rana et al. (2002)].

For imaging experiments the analogue atomiser is contained within a light tight, black anodised aluminium housing. Illumination is provided by a pulsed Nd:YAG laser with a wavelength of 532 nm, a typical energy of 90 mJ/pulse and a pulse duration of 6 ns. The laser light is converted into a 2 mm thick light sheet and fed into the interrogation area using an optical arm fitted with appropriate defocusing optics. The optical arm is positioned such that the centre of the light sheet is aligned with the centre of the melt nozzle. The short pulse duration provided by the laser allows particles to be ‘frozen’ even in exceptionally fast flows. The laser is capable of providing two pulses with a variable delay between the pulses of  $0.1 \mu\text{s} - 5 \text{ s}$ . These pulses are synchronised with the shutter of a high speed, 2 Mpixel camera. The output from the system is thus a pair of images with a user defined delay between the pair and a very short effective shutter speed. Imaging was conducted either normal to the central axis of the melt delivery nozzle, or inclined to it at an angle of  $35^\circ$ . Example images from both configurations are shown in Fig. 3.

A further consequence of the imaging technique is that by using appropriate software (in this case INSIGHT 3G<sup>‡</sup>), a velocity map can be created for individual droplets within the plume using the Particle Image Velocimetry (PIV) technique. This technique uses a cross-correlation algorithm to identify particles within the image pair that can be traced with a high degree of certainty from the first image to the second. Given a calibrated length scale in the image and the temporal separation between images, calculation of the particle velocity can then be undertaken. In many PIV applications tracer or seed particles are introduced into the flow, but in this work we have relied on the fact that the software is capable of detecting individual particles created by the break-up of the melt stream during atomisation. This will however inevitably lead to some biasing of the detection, with higher weighting being given to larger droplets which are easier to detect. Nonetheless, the technique provides valuable

<sup>‡</sup> INSIGHT 3G is a product of TSI Inc., Shoreview, MN, USA

information regarding the particle flow field. In order to ensure reliable tracking in the atomisation environment, which contains a high density of fast moving particles, the temporal separation of the images is short, typically 5  $\mu$ s.

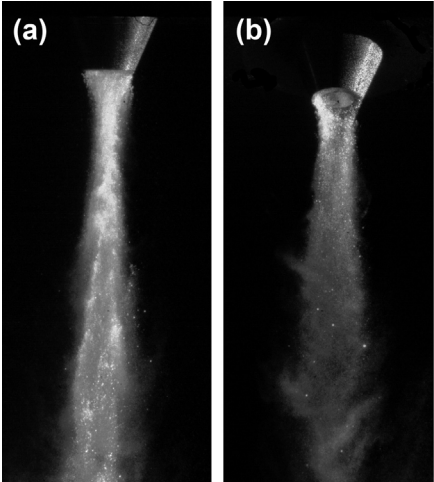


**Figure 3.** Example images of water atomisation obtained using the pulsed Nd:YAG laser system (a) normal to the atomiser axis and (b) offset from the normal by 35°.

**Results**

The aspiration characteristics of the four melt nozzles used in this study, as a function of the inlet gas pressure, are shown in Fig. 4. In all four cases the aspiration pressure is positive, i.e. the pressure at the melt delivery nozzle is above ambient. Such a positive aspiration is generally considered to have a negative influence on the smooth running of the gas atomiser as an excess pressure is required in the tundish to ensure the flow of melt. Moreover, fluctuations in the melt flow can result in ‘freeze off’ at the tip. Nonetheless, a positive aspiration pressure is a common feature of many close-coupled atomisers utilising an apex angle around 45° and this design is employed in a number of commercial systems. In the system described here a constant overpressure of 40 kPa was applied to the atomised fluid and, in the absence of this overpressure, no flow of the second fluid would result.

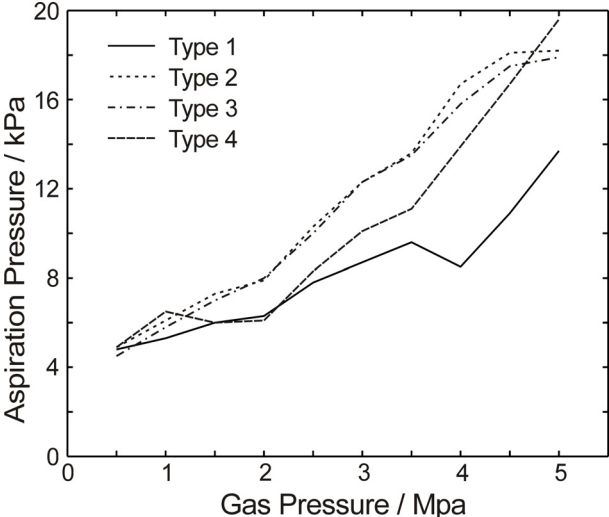


**Figure 4.** Aspiration pressure in the melt delivery tube 3 mm above the base of the nozzle as a function of inlet gas pressure for the four nozzle geometries studied here.

All nozzles display a strong, positive correlation between gas pressure and aspiration pressure, with very similar aspiration pressures of around 4 kPa being measured at the

lowest gas pressure studied (0.5 MPa). The two internally tapered nozzles (Types 2 & 3) show very similar aspiration characteristics, both showing a steeper gradient than the flat-tipped nozzle, such that the aspiration pressure for these nozzles is consistently higher than for the flat nozzle. The hemispherical (Type 4) nozzle shows somewhat more complex behaviour, with the relation between the gas and aspiration pressures possibly being non-linear. Below 2 MPa gas pressure the behaviour of the hemispherical is similar to that of the flat-tipped nozzle, but thereafter the aspiration pressure increases steeply with increasing gas pressure, finally exceeding that of the Type 2 & 3 nozzles above 4.5 MPa.

Fig. 5 shows a pair of images taken in the 35° orientation using the flared, Type 3 melt nozzle (no lip). This nozzle type was chosen as it has been shown to give one of the sharpest frequency peaks in a DFT analysis (Mullis et al.; 2008). It is clear from the two images in Fig. 5 that the melt 'plume' does indeed consist of a very fine filament undergoing precessional motion. In the 500  $\mu$ s interval between the two frames the filament moves from almost at the back of the nozzle (as viewed) to close to the front of the nozzle, somewhat over 120° in total. This is consistent with the 600 Hz precession frequency measured for this nozzle using the DFT methodology. This we believe constitutes direct observational evidence for the precession of the melt plume during close coupled gas atomisation.

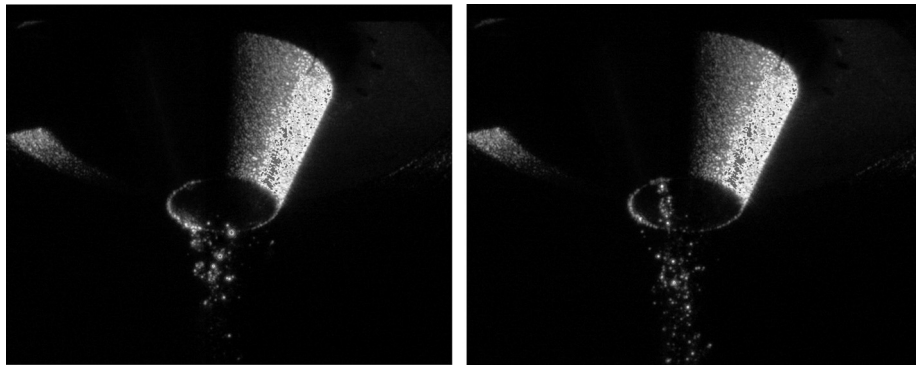


**Figure 5.** Two images, separated by 500  $\mu$ s, of the melt delivery nozzle during water atomisation clearly demonstrating precession of a thin melt filament.

In Fig. 5, a very narrow melt filament is shown to be associated with the flared type melt nozzle, which has been shown elsewhere to give a sharply peaked DFT spectrum. However, there are other atomiser configurations which give a far more diffuse DFT spectra, particularly when the melt delivery nozzle has a broad, flat tip as shown in Fig. 2b (Type 1). In order to better understand and interpret these diffuse spectra, atomisation experiments have been performed with three of the four nozzle geometries shown in Fig. 2b (the behaviour of the Type 3 and Type 4 nozzles is very similar so we do not reproduce the data here).

In each case the experiment has been filmed with the pulsed Nd:YAG system to obtain high quality still images, the results of which are shown in Fig. 6. Also shown for comparison are DFT spectra from McCarthy (2010). In order to facilitate more direct comparison between the three DFT spectra, each has been normalised to a peak spectral power of 1 and has been smoothed using the filter due to Savitzky and Golay (1964), with a kernel width of 25. This makes it possible to unambiguously determine the full width half maximum (FWHM) of the peak, which we determine for the three cases as (a-Type1) 1091 Hz, (b-Type 2) 145 Hz and (c-Type 4) 132 Hz, although in case (a) it is possible that this may be a superposition of more than one overlapping peak.

Two main observations may be made about the results. Firstly, it is clear that a sharply peaked DFT spectrum is associated with a narrow melt filament and that as the filament becomes more extensive the peak in the DFT spectrum becomes broader. Secondly, the

width of the melt filament appears to be directly linked to the shape of the melt delivery nozzle. Specifically, internal flaring of the melt nozzle appears to produce a very narrow, regular jet, whilst having a flat lip to the melt nozzle tends to produce a broad filament with a wider range of rotational frequencies being present. The extreme case of this is where the melt nozzle is completely flat, wherein a very broad melt plume is observed, covering a significant fraction of the circumference of the nozzle. The melt wetting pattern on such flat nozzles has been shown by Anderson et al. (2006) to be highly erratic, which is consistent with the wider range of frequencies observed in the DFT spectra. Using an internally hemispherical (Type 4) profile makes the melt filament narrower than is the case for the Type 2 nozzle, although only marginally so.

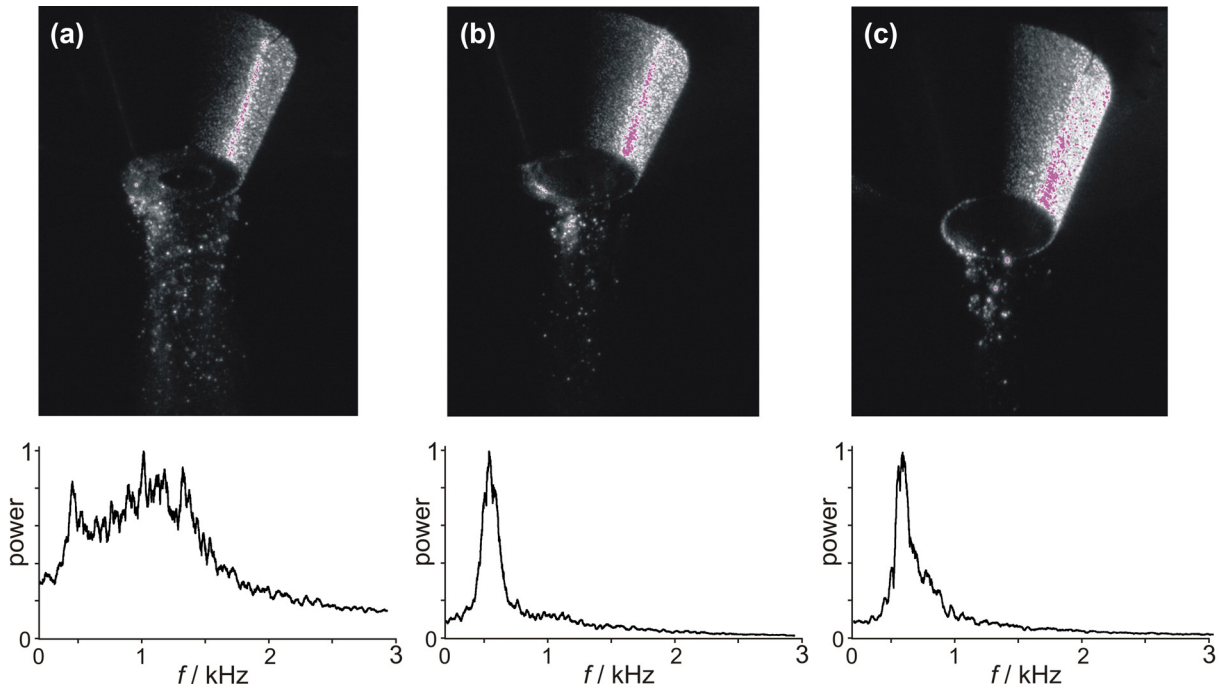


**Figure 6.** Correlation between the still image and the Fourier spectra for (a) flat-tipped, (b) flared and (c) hemispherical nozzles.

Further interpretation of the still image pairs produced by the pulsed laser system can be obtained by applying PIV mapping software. A typical image, with superimposed velocity field, obtained using this procedure is shown in Fig. 7. The melt delivery nozzle, the left hand side of which is in shadow, is clearly evident at the top of the image. The most obvious features from the image are also shown in sketch form to the right of the PIV image, although we have restricted this to the primary region close to the nozzle. Two dashed arrows show the approximate alignment of the gas jets, estimated from the die configuration. From this we have also indicated the geometric focus of the gas jets (i.e. the point at which the projection of the jets meet) although, as the gas is in choked flow, it will expand freely upon exiting the jet and, as such, the indicated focus is for reference only.

In the image the melt plume is displaced somewhat to the right. This is not unexpected given that we know that the plume is precessing. Indeed, even if the plume were to appear central in the 2-D image, the precession of the jet would mean that the actual melt plume would be off-axis, in this case either in front of, or behind, the central axis of the nozzle, with respect to the line of sight of the camera. Highly complex flow patterns, with many recirculation eddies, are evident, particularly downstream in the secondary atomisation zone.

From the image we have attempted to identify the ‘neck’ in the melt plume, that is, the point where the plume has its smallest diameter. In the literature this ‘neck’ region is often located coincident with the focus of the gas jets (see e.g. Ting et al., 2002). The free expansion of

the gas upon exiting the jet means that this is not the case here, with the neck appearing somewhat above the geometric focus of the gas jets. We suspect that the observed neck position probably corresponds to the location at which the expanding gas jet first impinges upon the melt stream, although this remains speculative as we do not have direct images of the gas flow-field in this case.

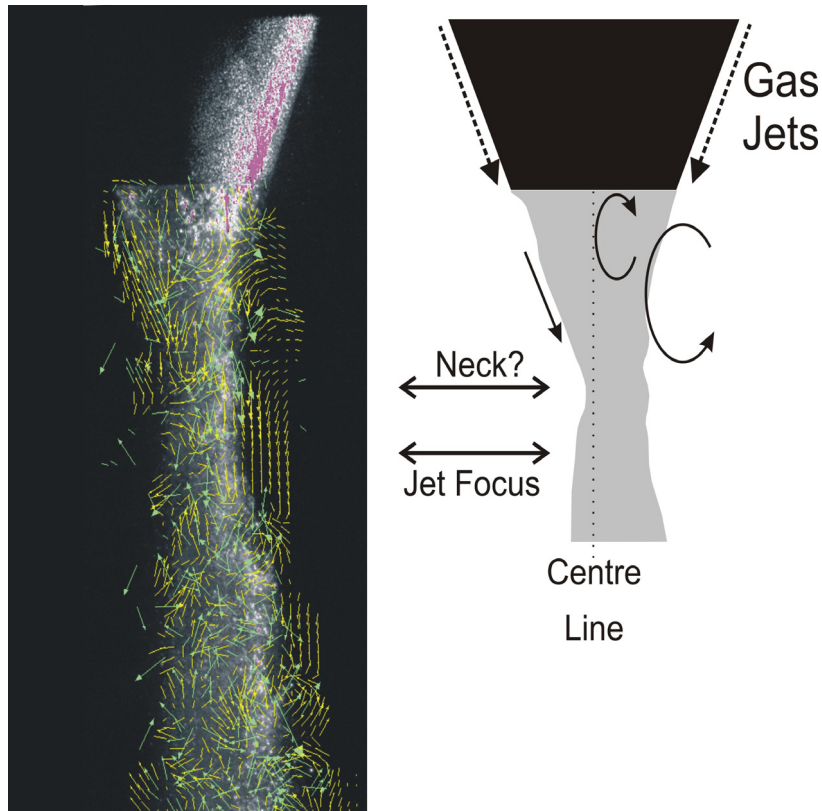


**Figure. 7.** Image of water atomisation with superimposed velocity vectors calculated using the PIV technique from an image pair with  $5 \mu\text{s}$  separation. The approximate trajectory of the gas jets is shown by the dashed lines. The focus of the jets and an apparent neck in the melt plume are also indicated.

We also note with interest the asymmetry in the flow pattern close to the nozzle in this region above the 'neck'. To the right of the image (where there is a greater volume of material being atomised) there is evidence of recirculation. Conversely, on the left hand side of the image, where there is a deficiency of material being atomised, there is a strong, laminar down-flow, with no evidence of recirculation. The lower extent of this circumferential recirculation eddy appears close to the 'neck' position. There is also, perhaps more tentative, evidence for recirculation within the melt plume. Evidence for such recirculation eddies has previously been presented by Mates & Settles (2005) on the basis of Schlieren imaging of the gas only flow. Generally a symmetrical pair of such eddies have been reported although only one is evident here. We are not clear at this time as to whether this indicates that only one such eddy is present or whether the high density in the spray has inhibited imaging.

## Discussion

It is clear from the results presented above that the melt spray cone is actually comprised of a jet precessing around the surface of a cone and that the morphology of this jet is heavily influenced by the geometry of the melt delivery nozzle. A nozzle with a broad flat tip produces a wide jet with a rotational motion that appears to be highly irregular, a wide range of frequencies being present in the corresponding DFT spectra. We believe that the broad range of frequencies present probably arises due to differential movement of the leading and trailing edges of the pre-filming area. This then would be an inherent feature of having a

broad jet, as there is no obvious mechanism to keep the leading and trailing edges synchronised. This is also consistent with the rather irregular pre-filming patterns observed by Anderson et al. (2006), attributed to irregular wetting of the nozzle by the melt. Conversely, nozzles with an internal flare or taper produce a much finer jet and, from the DFT spectra, we would deduce that its precessional motion is highly regular. The regularity of this motion we believe indicates both that the precession is steady and that the filament remains well collimated, with minimal differential movement of the leading and trailing edges.

The behaviour of internally profiled nozzles (Types 2, 3, & 4) thus appears to be fundamentally different to the irregular wetting behaviour seen with the flat tipped nozzle and we postulate that a different physical mechanism may be giving rise to the well collimated jet. Nozzles of the internally tapered and hemispherical types were developed to improve coupling between the gas and the melt and the subsequent disruption of the latter. We suggest that this closer coupling to the gas field may exist and results in recirculation eddies that focus the melt flow into well defined, highly collimated channel(s). This may be a consequence of these eddies penetrating up into the internal void in the nozzle (see Fig. 8).

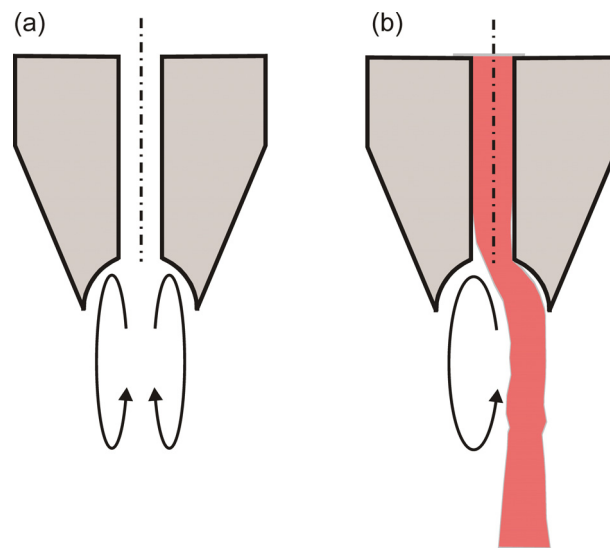


**Figure. 8.** Proposed model for melt collimation into filaments in tapered and concave nozzles, showing (a) gas only flow in which recirculation eddies penetrate into the nozzle cavity and (b) two-phase flow in which the melt path is determined by ‘easy’ paths between eddies.

Although somewhat speculative, this model does give rise to a prediction. If the melt is being channelled by the gas flow, this should be independent of the wetting behaviour of the fluid. As such the FWHM of the DFT spectra should show no dependence on the surface tension of the melt. This is difficult to investigate with metal, as changing the atomised melt to alter the wetting behaviour is likely to lead to a consequential change in a range of other parameters. However, in the analogue atomiser wetting behaviour can be altered by the addition of a surfactant. The FWHM in the DFT spectra for the centre position of the plume as a function of the surface tension of the second fluid, which is being atomised with a Type 2 nozzle, is shown in Fig. 9. These results appear to indicate a strong  $\sigma$  dependence for  $\sigma > 60 \text{ mN m}^{-1}$  but virtually no dependence for  $\sigma < 50 \text{ mN m}^{-1}$ . This we believe is consistent with the proposition that the melt is being collimated by gas eddies. At low surface tensions the FWHM of the spectra tends to an asymptotic value around 205 Hz, and we note that this is around a factor of 4 smaller than that observed for the flat-tipped, Type 1 nozzle. This we believe offers strong evidence that the effect being observed is not simply irregular wetting. However, we suggest that at high values of the surface tension there is a supplementary effect from the surface tension which tends to pull the melt filament into a more tightly

collimated jet. At lower values of the surface tension this effect is absent and the effect of gas only collimation is observed.

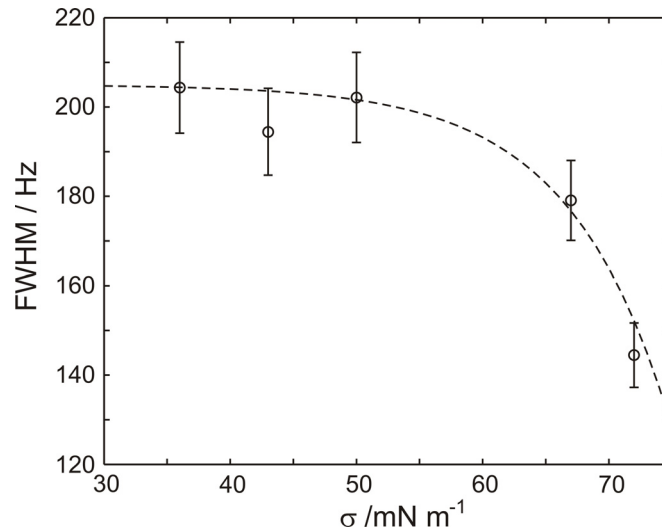


**Figure. 9.** Dependence of the FWHM in the DFT spectra of the plume centre position,  $\bar{j}$ , as a function of the surface tension of the atomised fluid.

Interestingly, the trend in many commercial atomisers and in the literature on discrete jet atomisers is towards internally flared melt nozzles with either minimal or no lip. The results presented here suggest that this accentuates the inhomogeneity in the wetting of the melt nozzle tip but makes the behaviour of the resulting melt filament correspondingly more regular (i.e. the resulting filament is finer, but it is precessing in a more regular manner). As the effective (instantaneous) value of  $G$  will depend upon the width of the filament, the likely upshot of this is that a melt delivery nozzle with a pronounced internal taper will produce a more uniform product, with the melt filament always being exposed to a similar number of gas jets, but with a lower overall efficiency than a flat melt nozzle in which the broader but more erratic melt filament is exposed to a larger, but more variable number of gas jets. Other strategies, such as milling of slots in the tip of the melt delivery nozzle, have been reported by Anderson et al. (2006), which aim to improve the efficiency and uniformity of melt delivery by channelling the melt towards the gas jets. Of course, in all cases low frequency pulsation in the quantity of the melt being delivered to the nozzle of the atomiser due to the open- to closed-wake transition will cause a variation in  $G$  which will be superimposed upon any variation due to erratic wetting of the nozzle.

Results from the PIV analysis suggest that there is a strong coupling between the melt and gas flow fields. Specifically, the asymmetry in the melt flow field brought about by the precession of the melt plume is mirrored in the gas flow field, with a circumferential recirculation eddy apparent where the melt plume is closer to the gas jets and a strong down-flow where it is further away from these jets. Although Ting et al. (1998) have previously postulated the existence of recirculation eddies at the circumferential edge of the gas-melt interface in the primary atomisation zone, we believe that this is the first evidence for a strong asymmetry in this type of structure and is indicative of the strong coupling between the melt and gas flow field. Of course, given that the melt plume is precessing with a frequency of several hundred Hertz, it must be assumed that the observed asymmetry in the gas flow field is varying on a commensurate time-scale.

### Summary and Conclusions

We have used a defocused, pulsed Nd:YAG laser to produce pairs of still images during close-coupled gas atomisation with an effective shutter speed of 6 ns, and these images have subsequently been used to reconstruct the velocity field within the atomisation plume

using the Particle Image Velocimetry technique. The information thus obtained has been used to supplement the interpretation of previous studies into CCGA using high frame rate (18,000 fps) video imaging coupled with quantitative Fourier analysis. The main outcomes of this work are:

- it is unambiguously demonstrated that the spray cone during CCGA actually consists of a thin jet precessing around the surface of a cone,
- the morphology of this jet is strongly influenced by the geometry of the melt nozzle, with flat tipped nozzles giving a broad jet while nozzles with an internal taper give a fine, well collimated filament,
- for low values of the surface tension in the second fluid the nature of the filament is independent of the actual value of the surface tension, suggesting that this effect is not solely related to wetting behaviour,
- the asymmetry that is produced by the precession of the melt filament appears to be transferred to the gas flow-field, which displays circumferential eddies on the side in which the atomised fluid is closest to the gas but not on the opposite side.

## References

- Anand, V., Kaufman, A.J. and Grant, N.J., 1978. Rapid solidification of a modified 7075 aluminium alloy by ultrasonic gas atomization. In: *Rapid Solidification Processing, Principles & Technologies II* (Eds. Robert Mehrabian, B. H. Kear, M. Cohen), Claitor, Baton Rouge, LA, pp. 273-286.
- Anderson, I.E., Figliola, R.S. and Morton H., 1991. Flow mechanisms in high pressure gas atomization. *Mater. Sci. Eng. A* 148, 101-114.
- Anderson, I.E., Peretti, M., Conin, J.A. and Figliola, R.S., 2006. Visualisation of enhanced primary atomization for powder size control. *Proc. 3rd Int. Conf. on Spray Deposition and Melt Atomisation*, Bremen, CD-proceedings.
- Anderson, I.E. and Terpstra, R.L., 2002. Progress toward gas atomization processing with increased uniformity and control." *Mater. Sci. Eng. A* 326, 101-109.
- Anderson, I.E., Terpstra, R.L., Figliola, R.S., 2004. Melt feeding and nozzle design modifications for enhanced control of gas atomisation, *Advances in powder metallurgy and particulate materials. Adv. Powder Metall. Part. Mater.*, part 2, 26-36.
- Bradley, D., 1973. On the atomisation of a liquid by high velocity gases: Parts 1 and 2. *J. Phys. D: Appl. Phys.* 6, 1724-1736 and 2267-2272.
- Klov, E. and Schfer, W.M., 1972. *High Pressure Gas Atomisation of Metal*, 57, Syracuse, Syracuse University Press, pp. 57.
- Lubanska, H., 1970. Correlation of spray ring data for gas atomization of liquid metals. *J. Metals* 22, 45-49.
- Mates, S.P. and Settles, G.S., 1996. High-Speed Imaging of Liquid Metal Atomization by Two Different Close-Coupled Nozzles. *Adv. Powder Metall. Part. Mater.*, part 1, 67.
- Mates, S.P. and Settles, G.S., 2005. A study of liquid metal atomization using close-coupled nozzles, Part 2: Atomization behaviour. *Atomization and Sprays* 15, 41-59.
- McCarthy, I.N., Aslam, Z., Adkins, N.J., Mullis, A.M. and Cochrane, R.F., 2009. High speed imaging and Fourier analysis of the melt plume during close-coupled gas atomisation. *Powder Metall.* 52, 205-212.
- McCarthy, I.N., 2010. *Optical Investigations into Close-Coupled Gas Atomisation*, PhD thesis, University of Leeds.
- Miller, S.A., 1986. Apparatus for melt atomization with a concave melt nozzle for gas deflection, United States Patent 4619597.
- Mullis, A.M., Adkins, N.J., Aslam, Z., McCarthy, I.N. and Cochrane, R.F., 2008. High frame rate analysis of the spray cone geometry during close-coupled gas atomization. *Int. J. Powder Metall.* 44, 55-64.
- Nasr, G.G., Yule, A.J. and Bendig, L., 2002. *Industrial sprays and atomisation design: Analysis and applications*, Springer Publishing pp. 494.
- Rana, D., Neale, G.H. and Hornof, V., 2002. Surface tension of mixed surfactant systems: lignosulfonate and sodium dodecyl sulfate. *J. Colloid Polym. Sci.* 280, 775-778.

- Savitzky, A., & Golay, M.J.E., 1964. Smoothing and differentiation of data by simplified least squares procedures. *Analytical Chem.* 36 1627-1639.
- Ting, J., Anderson, I.E., Terpstra, R.L. and Mi, J., 1998. Design and testing of an improved convergent-divergent discrete-jet high pressure gas atomization nozzle. *Adv. Powder Metall. Part. Mater.*, part 10, 13.
- Ting, J., Connor, J. and Ridder, S., 2005. High-speed cinematography of gas-metal atomization. *Mater. Sci. Eng. A* 390, 452-460.
- Ting, J., Peretti, M. and Eisen, W.B., 2002. The effect of wake-closure phenomenon on gas atomization performance. *Mater. Sci. Eng. A.* 326, 110-121.
- Ünal, A., 1989. Influence of gas flow on performance of "confined" atomization nozzles. *Metall. Trans. B* 20, 833-843.
- Unal, R., 2007. Improvements to close coupled gas atomisation nozzle for fine powder production. *Powder Metall.* 50, 66-71.